Supporting Information

Deep Ultraviolet Luminescence Due to Extreme Confinement in Monolayer GaN/Al(Ga)N Nanowire and Planar Heterostructures

Anthony Aiello[1], Yuanpeng Wu[1], Ayush Pandey[1], Ping Wang[1], Woncheol Lee[1], Dylan Bayerl[2], Nocona Sanders[2], Zihao Deng[2], Jiseok Gim[2], Kai Sun[2], Robert Hovden[2], Emmanouil Kioupakis[2], Zetian Mi[1], and Pallab Bhattacharya[1]

[1]Department of Electrical Engineering and Computer Science, University of Michigan,

1301 Beal Avenue, Ann Arbor, MI 48109-2122, USA

[2]Department of Materials Science and Engineering, University of Michigan,

Ann Arbor, MI 48109, USA

The supporting information contains 9 pages in support of the main text. It discusses 3 topics:

1. Computational Details of Electronic and Optical Gaps
2. Additional TEM images of planar GaN monolayers
3. XRD of $Al_{0.65}Ga_{0.35}N$ barrier

1. Computational Details:

We investigated the electronic and excitonic properties of a monolayer GaN quantum well embedded in Al(Ga)N barriers using first-principles calculations based on density functional theory (DFT) and many-body perturbation theory. First, we obtained the lattice parameters of AlN and GaN from DFT structural relaxation calculations, using local density approximation (LDA) for the exchange-correlation functional within the Quantum ESPRESSO code [S1-S3]. For structural relaxations we used norm-conserving pseudopotentials including 4s, 4p, and 3d electrons of Ga in the valence, as the 3d electrons are needed to obtain accurate lattice constants in the group-III nitrides [S4]. Using the relaxed lattice parameters, we built a supercell consisting of a monolayer GaN separated by Al(Ga)N layers. We enforced the in-plane lattice parameters to be constant and only allowed ions to move along the c-axis for the supercell structural relaxation.

Band-structure DFT calculations were performed on 4x4x1 Monkhorst-Pack mesh for $(Al_{0.67}Ga_{0.33}N)_9$-$(GaN)_1$ structure and 8x8x1 Monkhorst-Pack mesh for $(AlN)_9$-$(GaN)_1$ structure. We used norm-conserving valence pseudopotentials which consider 4s and 4p electrons as valence electrons. A plane-wave cutoff energy of 70 Ry converged the total energy to within 1 mRy/atom. Compared to GW calculations with the semicore Ga pseudopotentials, which treat the 3s, 3p, and 3d electrons of Ga as valence electrons, the valence Ga pseudopotential overestimates the bandgap of the investigated structures by an amount in the range of 0.22-0.27 eV while reducing the computational cost of the large-size super-cell simulation. In the following quasiparticle calculations for the monolayer GaN/Al(Ga)N heterostructures we employ the valence Ga pseudopotential and reduce our calculated gaps by the corresponding amount that

corrects the discrepancy between the band gaps of the valence pseudopotential and the more accurate semicore pseudopotential calculations.

The quasi-particle band structure is calculated by the G_0W_0 method, as implemented in the BerkeleyGW package [S5]. We employed the generalized plasmon-pole model for the calculation of frequency-dependent dielectric effects [S6] and the static-remainder approach to accelerate the convergence over unoccupied states [S7]. The screening cutoff energy of 20 Ry and the number of bands up to 50 % of the screening cutoff converged the quasi-particle band gap to 0.05 eV. Finally, to obtain exciton-binding energy, the Bethe-Salpeter equation (BSE) method was employed within BerkeleyGW. The top two degenerate valence states and the lowest conduction state were included in the exciton calculations. For the $(Al_{0.67}Ga_{0.33}N)_9$-$(GaN)_1$ structure, a 20x20x5 Brillouin-zone-sampling grid is sufficient to converge the exciton binding energy to within 10 %, while for the $(AlN)_9$-$(GaN)_1$ structure similar convergence is achieved with a 48x48x6 sampling grid.

Next, to explore the effects of carrier localization by barrier alloy disorder and to check the validity of the results obtained from the supercell structure with ordered alloy barriers, we compared three models (ordered alloy structure, special quasi-random structure (SQS) [S8-S9], and five different random alloy structures) for the $Al_{0.67}Ga_{0.33}N$ barrier. We expanded a $(\sqrt{3} \times \sqrt{3})R60^{\circ}$ unit cell into a 2x2x2 supercell to build $(Al_{0.67}Ga_{0.33}N)_3(GaN)_1$ structures with three different alloy models. Then we performed DFT structural relaxation for each structure using the norm-conserving pseudopotential of Ga, which includes 4s, 4p, and 3d electrons as its valence. We used a plane-wave cutoff energy of 90 Ry and included only the Γ point.

After structural relaxations, we performed DFT calculations using the norm-conserving pseudopotential of Ga that includes valence 4s and 4p electrons. We adopted a plane-wave cutoff energy of 70 Ry and 2x2x2 Monkhorst-Pack mesh. Figure S1 shows the electron and hole wave functions of the SQS, while Table S1 summarizes the conduction band minimum, valence band maximum, and the bandgap of $(Al_{0.67}Ga_{0.33}N)_3(GaN)_1$ structures with different alloy configuration.

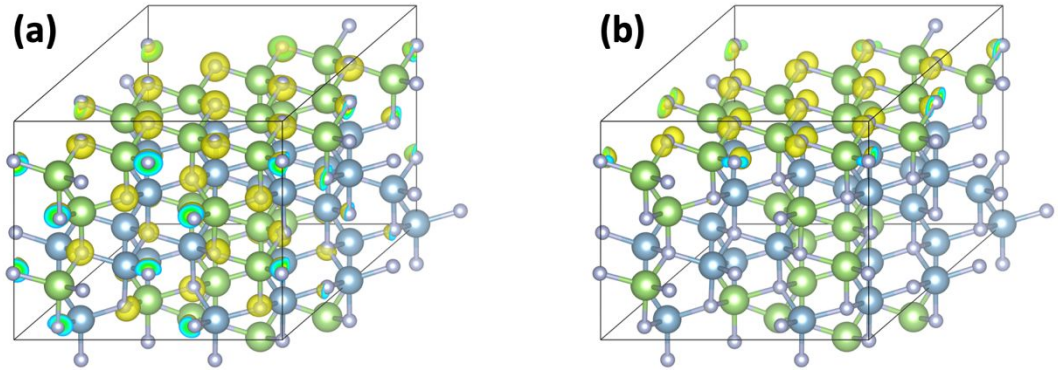

Figure S1: 3D isosurface plot of (a) electron wave function and (b) hole wave function of the special quasi-random $Al_{0.67}Ga_{0.33}N$ barrier structure. The isovalue is chosen to be 15% of the maximum.

Table S1: Summary of the DFT electron and hole energies of $(Al_{0.67}Ga_{0.33}N)_3(GaN)_1$ supercell structure based on different models for AlGaN barriers.

Type of $Al_{0.67}Ga_{0.33}N$ barrier structure	Conduction band minimum	Valence band maximum	Band gap
Ordered alloy structure	9.935	6.734	3.201
Special quasirandom structure	9.929	6.744	3.185
Random alloy structure 1	9.924	6.744	3.181
Random alloy structure 2	9.926	6.739	3.187
Random alloy structure 3	9.931	6.744	3.187
Random alloy structure 4	9.924	6.745	3.179
Random alloy structure 5	9.924	6.744	3.180
Statistics for 5 random alloy structures	9.928 ± 0.003	6.740 ± 0.002	3.188 ± 0.004

2. TEM Images of planar GaN monolayers

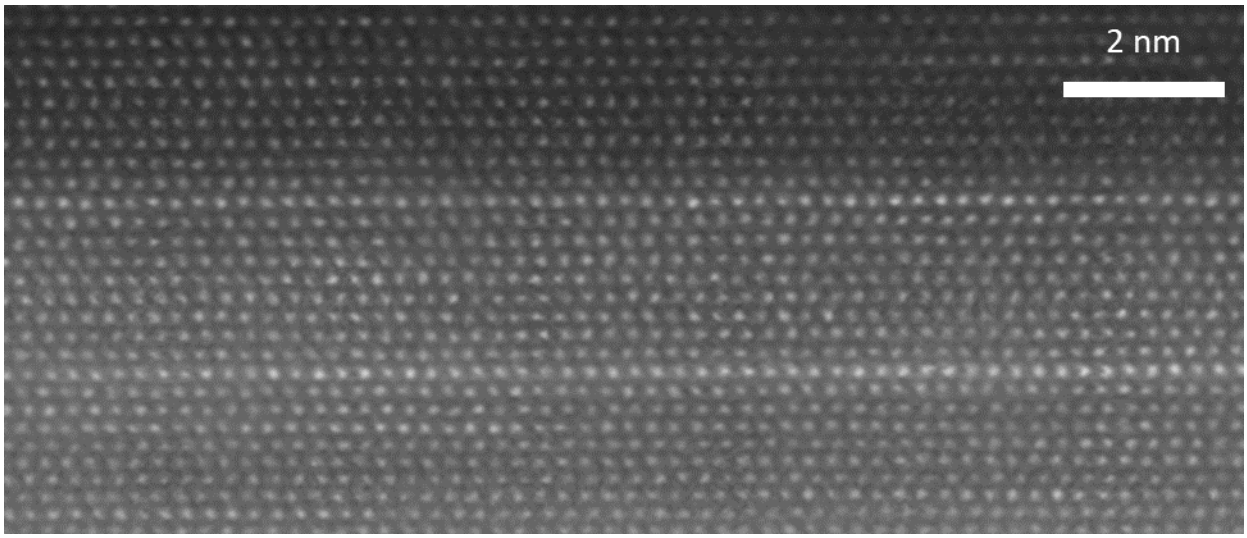

Figure S2: ADF-TEM image of a 2-period planar GaN/AlGaN monolayer structure under similar growth conditions as the single period.

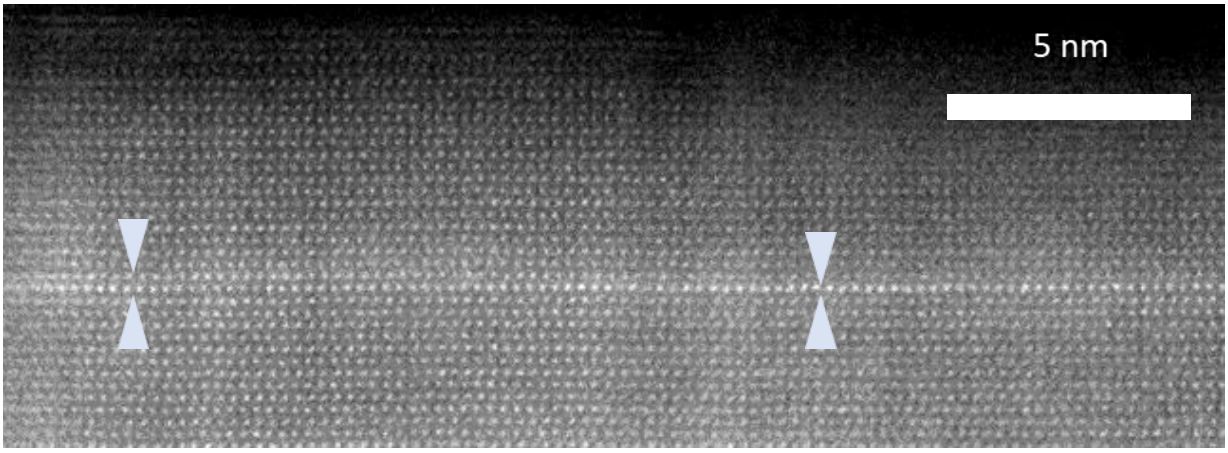

Figure S3: HAADF-TEM image of the single GaN monolayer. Arrows indicate interface roughness, which is expected for these planar layers with large lateral extent, as opposed to nanowires, which may vary 1-2 ML.

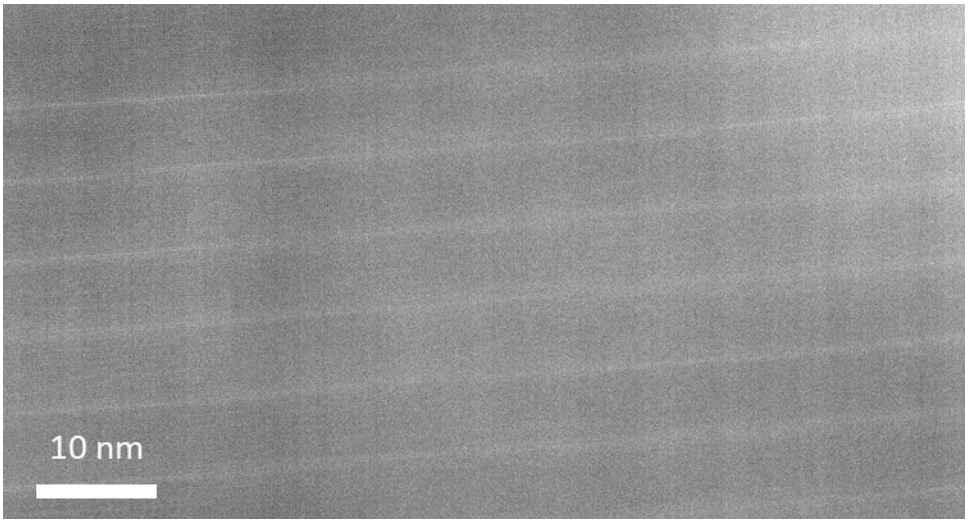

Figure S4: HAADF-TEM image of a heterostructure with multiple GaN/$Al_{0.65}Ga_{0.35}N$ periods. Growth conditions and substrate are identical to that of the single period sample in this study.

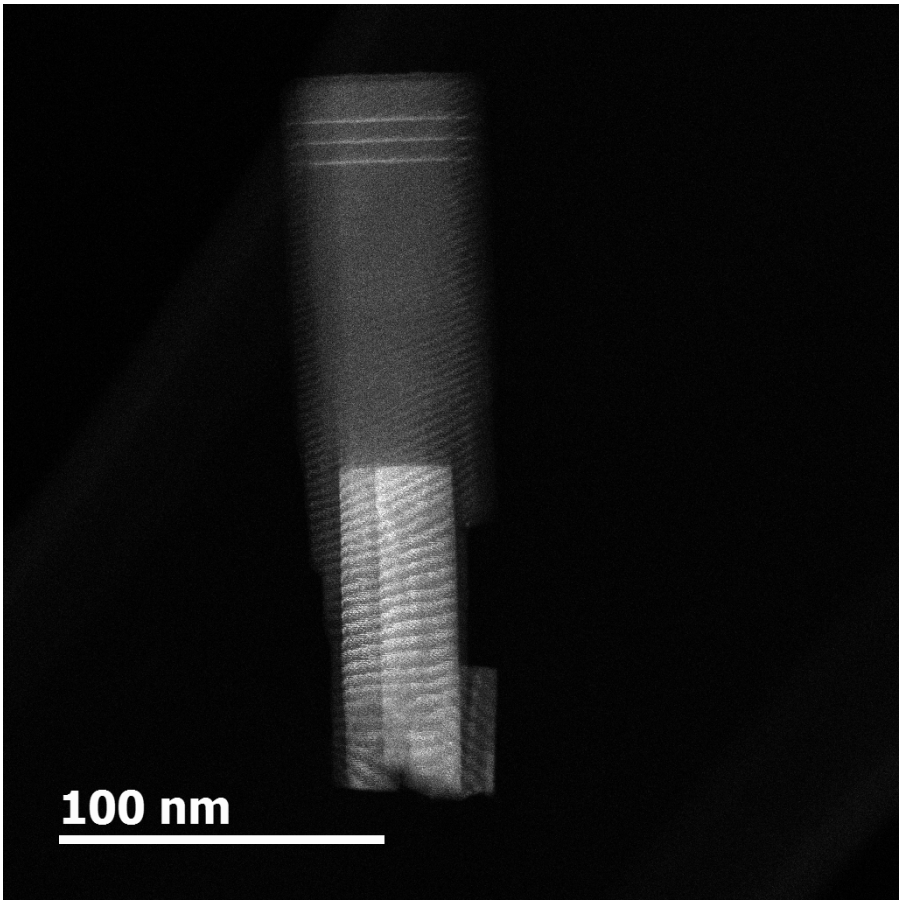

Figure S5: TEM image of a single nanowire with 3 GaN monolayer periods used in this study.

3. XRD of $Al_{0.65}Ga_{0.35}N$ barrier of planar structure

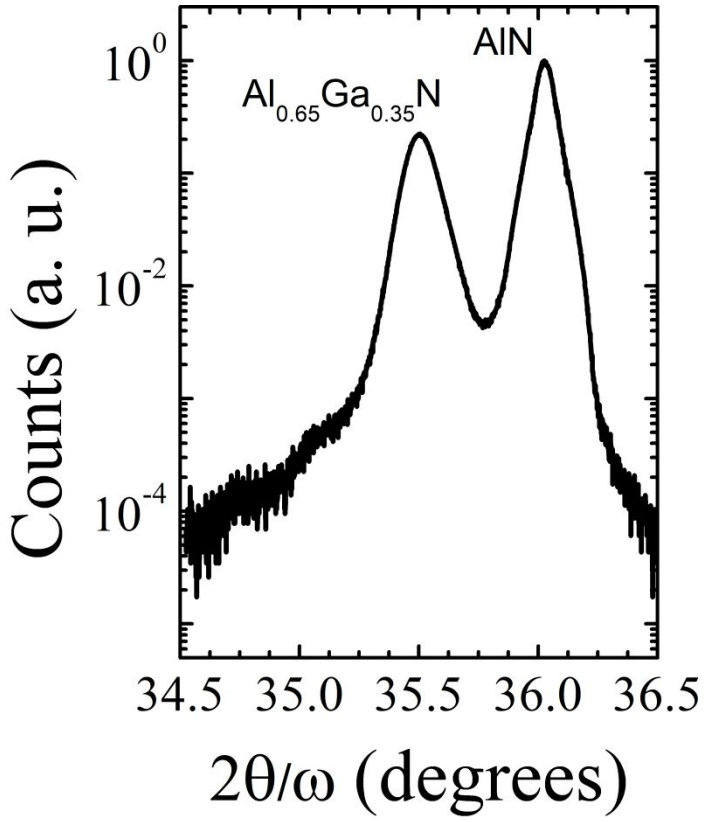

Figure S6: XRD rocking curve of $Al_{0.65}Ga_{0.35}N$ epitaxially-grown on AlN/sapphire substrate under identical growth conditions as the planar sample in this study.

References:

(S1) Ceperley, D.M.; Alder, B.J. Ground State of the Electron Gas by a Stochastic Method. *Phys. Rev. Lett.* **1980**, *45*, 566–569.

(S2) Perdew, J.P.; Zunger, A. Self-Interaction Correction to Density-Functional Approximations for Many-Electron Systems. *Phys. Rev. B* **1981**, *23*, 5048-5079.

(S3) Giannozzi, P.; Baroni, S.; Bonini, N.; Calandra, M.; Car, R.; Cavazzoni, C.; Ceresoli, D.; Chiarotti, G.L.; Cococcioni, M.; Dabo, I.; Dal Corso, A.; De Gironcoli, S.; Fabris, S.; Fratesi, G.; Gebauer, R.; Gerstmann, U.; Gougoussis, C.; Kokalj, A.; Lazzeri, M.; Martin-Samos, L.; Marzari, N.; Mauri, F.; Mazzarello, R.; Paolini, S.; Pasquarello, A.; Paulatto,

L.; Sbraccia, C.; Scandolo, S.; Sclauzero, G.; Seitsonen, A.P.;Smogunov, A.; Umari, P.; Wentzcovitch, R.M. QUANTUM ESPRESSO: A Modular and Open-Source Software Project for Quantum Simulations of Materials. *J. Phys.: Condens. Matter* **2009**, *21*, 395502.

(S4) Stampfl C.; Van de Walle, C.G. Density-Functional Calculations for III-V Nitrides Using the Local-Density Approximation and the Generalized Gradient Approximation. *Phys. Rev. B* **1999**, *59*, 5521–5535.

(S5) Deslippe, J.; Samsonidze, G.; Strubbe, D.A.; Jain, M.; Cohen, M.L.; Louie, S.G. BerkeleyGW: A Massively Parallel Computer Package for the Calculation of the Quasiparticle and Optical Properties of Materials and Nanostructures. *Comput. Phys. Commun.* **2012**, *183*, 1269-1289.

(S6) Hybertsen, M.S.; Louie, S.G. Electron Correlation in Semiconductors and Insulators: Band Gaps and Quasiparticle Energies. *Phys. Rev. B* **1986**, *34*, 5390–5413.

(S7) Deslippe, J.; Samsonidze, G.; Jain, M.; Cohen, M.L.; Louie, S.G. Coulomb-Hole Summations and Energies for GW Calculations with Limited Number of Empty Orbitals: A Modified Static Remainder Approach. *Phys. Rev. B* **2013**, *87*, 165124.

(S8) Zunger, A.; Wei, S.-H.; Ferreira, L. G.; Bernard, J. E. Special Quasirandom Structures. *Phys. Rev. Lett.* **1990**, *65* (3), 353–356.

(S9) van de Walle, A.; Tiwary, P.; de Jong, M.; Olmsted, D. L.; Asta, M.; Dick, A.; Shin, D.; Wang, Y.; Chen, L.-Q.; Liu, Z.-K. Efficient Stochastic Generation of Special Quasirandom Structures. *CALPHAD: Comput. Coupling Phase Diagrams Thermochem.* **2013**, *42*, 13–18.